Low-energy excitonic resonances in metals. I. Experiments on divalent atoms

M. H. Bakshi, G. A. Denton, C. P. Flynn, J. C. Boisvert, and A. B. Kunz
Department of Physics and Materials Research Laboratory, University of Illinois at Urbana—Champaign, Urbana, Illinois 61801
(Received 29 October 1984)

We report differential ellipsometric measurement of optical constants for impurities in dilute alloys. For Mg, Zn, and Ca impurities in Li metal an impurity-specific absorption feature occurs in the (2—3)-eV range, superposed on an impurity-induced Drude background. The peaks are the $ns^2 \rightarrow nsnp$ excitations of the free divalent atoms, red-shifted by metallic screening. These are identified as low-energy excitonic resonances in which the photoexcited electron and hole linger together in the impurity cell under their mutual interaction. Single-particle approximations to the optical properties cannot reproduce these explicit two-carrier effects. The three species exhibit different behaviors with increasing composition. For Mg impurities, the resonance can be followed across the entire Li-Mg phase diagram, where in pure Mg metal it becomes the "interband transition." We infer that an excitonic resonance enhances the interband process. The following paper explores the explicit consequences of the electron-hole interaction, using a many-electron approach to small clusters, which appears to confirm the experimental deductions.

I. INTRODUCTION

In this paper we describe experimental investigations of optical excitations of metals. The experiments are interpreted to show that the interaction between the photoexcited electron and hole quasiparticles in the final state plays an important role in determining the excitation spectrum. In short, the optical response of the metal is modified by strong excitonic resonance-enhancement effects. In a companion paper that follows (hereafter referred to as paper II) these same phenomena are investigated by theoretical methods which make use of cluster calculations.[1]

Phenomena related to final-state interactions between electrons and holes are more widely recognized for insulating solids than for metals.[2–5] The long-range Coulomb interaction between two carriers having opposite signs gives rise to an infinite (in principle) spectrum of bound-pair states in an otherwise perfect insulator. Low-energy *un*bound configurations of the two carriers also possess wave functions which have enhanced amplitudes for small interparticle separations. The improved electron-hole overlap causes an enhancement of the low-energy continuum of optical interband transitions. Thus the optical spectrum of insulators is modified by the sharp lines of transitions to bound-pair states (excitons) and by increased low-energy interband absorption (excitonic enhancement). These phenomena in nonmetals have become progressively better understood since the first comprehensive model calculations were published by Elliott.[6]

In metals and alloys, which are the systems of concern here, the conduction electrons screen out the long-range interaction between quasiparticles, and so eliminate the infinite spectrum of bound-excitonic states. We note, in addition, that if the remaining interaction were strong enough to pull a bound exciton off an interband transition, the resulting exciton must be degenerate with the continuum of unbound electron-hole—pair states which, in a metal, extend from zero to all higher energies. Accordingly, the exciton would simply appear as a resonance in the continuum, with a width dependent on the Coulomb matrix element connecting the exciton to the unbound continuum. Any truly stable excitons, having a total energy less than the ground configuration, would signal a catastrophic instability of the normal ground state.

These factors have largely discouraged searches for excitonic effects in metals. Early efforts to discuss such effects were made by Phillips[5] and by Cohen.[7] An early paper by Mahan also discussed phenomena similar to those observed in the present investigations.[8] In the 1970s there appeared discussions of electron-hole coupling in conducting systems possessing strong space quantization or strong Landau quantization.[9] More recently, two of us have published a theory of excitonic enhancement of optical spectra of pure metals.[10] A calculation leading to the prediction of *bound* excitons in Al metal has also appeared.[11]

The experimental results for metals and alloys reported in this paper focus direct attention on the interaction between the electron and the hole in the photoexcited final state. Our results indicate that the electron-hole overlap is increased significantly by the forces acting between the two quasiparticles; their coupled motion persists for an appreciable time interval before they decay into independent quasiparticles propagating through the metal. This is an excitonic resonance which enhances the strength of some low-energy optical transitions. We find that these processes occur widely under favorable conditions in dilute alloys, and have previously been observed but not identified.[12–15] The impurity field presumably helps to localize one or both carriers in the impurity cell where their mutual interaction augments the overlap still further. What results are impurity-specific features of the alloy excitation spectra with oscillator strengths comparable with those of the analogous transitions of the impurity as

a free atom. In at least one case the process can be tracked across the entire alloy concentration range from the dilute impurity to the pure metal. Sharp features in the spectra of pure divalent metals have previously been regarded as interband transitions lacking enhancement.[16–25]

We emphasize the distinction between the enhanced process and the model ordinarily employed to describe the optical properties of alloys.[26–28] Extended single-particle orbitals $\psi(r)$ are calculated by some mean-field method such as the coherent potential approximation.[29,30] The optical strength is given in terms of a joint density of initial and final one-particle states:

$$\alpha(\hbar\omega)=\int_{E<E_F}\rho_1(E)\rho_2(E+\hbar\omega)\times|\langle\psi_1(E)|\,\mathbf{A}\cdot\mathbf{p}\,|\psi_2(E+\hbar\omega)\rangle|^2,$$

with ρ_1 the density of states, ψ_1, at $E<E_F$, and ρ_2 the density of states, ψ_2, at $E+\hbar\omega$, above E_F. Excitonic enhancements are explicitly absent from such calculations because the states ψ_1 and ψ_2 are dynamically independent, the electron wave function being calculated in the absence of the hole and vice versa.

Direct account of a *static* electron-hole interaction is taken in calculations of excitation profiles for *deep* core holes.[31] The deep hole is assumed to be stationary, and the electronic problem is solved in separate self-consistent calculations with and without the hole; optical spectra can then be calculated from matrix elements connecting the two configurations[32,33] (ΔSCF theory, where ΔSCF denotes self-consistent-field change). For metals this leads to the famous "x-ray-edge" problem. The predicted spectra occur at an energy generally dependent on the particular core hole and have shapes fixed by the local electronic structure. Observed spectra are indeed core-specific, but are more strikingly characteristic of the impurity structure, much more so than the static electron-hole coupling of ΔSCF theory can reproduce. This is the case in the simplest systems, such as, for example, halogen,[34] rare-gas,[35] and alkali-metal[36] impurity spectra in alkali-metal host lattices.[37]

In the low-energy regime one could obtain similarly sharp, impurity-specific spectra if the hole created in the excitation were to localize on the impurity center itself. Since metals necessarily maintain electrical neutrality, a hole localized for a time longer than the plasmon period would become screened by a local accumulation of neutralizing electrons. The screening deformation thus produces the same type of static electron-hole coupling that occurs in the deep-hole problem, and a ΔSCF theory (see, e.g., paper II) would doubtless exhibit impurity-specific spectra for shallow levels also. We wish to note, in particular, that the presence of the screening electrons can possibly act to trap an otherwise mobile hole on the excited center, so that the two-particle localization can occur cooperatively even in the absence of localized single-particle states. In both cases the overall result is that an electron and hole linger together at the impurity. The presence of sharp impurity-specific spectra therefore does not immediately determine whether or not the hole state is independently localized. That question can be settled only by comparison with single-particle predictions.

It is worth noting that "virtual-bound-state" theories of absorption have been employed to predict sharp structure for impurities which bind electrons in a sharp virtual level below E_F.[38–40] The d levels of transition-metal impurities provide examples of this behavior.[41–45] These theories explicitly neglect the electron-hole interaction (the two-particle Green's function is taken to be the product of two single-particle Green's functions).[39,40] In these theories, sharp structure in the predicted response is caused instead by transitions from the virtual level to propagating states immediately above E_F, rather than to an excited local configuration of two interacting carriers. To the extent that the level width is much less than the plasmon frequency, so that an unscreened hole lingers for a time longer than the plasmon period, the fundamental basis of the virtual-bound-state model in terms of local self-consistency seems open to serious question.

In the experimental work described below, the $ns^2\rightarrow nsnp$ transitions of divalent atoms were selected for investigation. Their oscillator strengths are large,[46] and these systems avoid the complexity of transition-metal behavior. The atomic transitions, which lie in the (4–8)-eV range,[47] are expected to red-shift in the metal. Alkali metals were chosen as host lattices for their simplicity, but, in practice, only experiments with Li metal were really successful. These matters are discussed in Sec. II of this paper, where experimental results are also presented. A preliminary account of the behavior of dilute alloys was published earlier,[48] and attention has been drawn to the consequences of the results for pure divalent metals.[49,10]

II. EXPERIMENTS

A. Apparatus

The measurements reported in this paper are ellipsometric determinations of optical constants made by polarization-modulation techniques. Samples were prepared by molecular-beam methods *in situ* at liquid-He temperatures to inhibit thermal evolution of the alloys.

Ellipsometric measurements were made using an automated photoelastic modulator employing the basic configuration proposed by Jasperson and co-workers.[50] In this technique the light is first polarized by a Glan-Taylor prism. It then passes through an oscillating quartz bar, which phase-modulates the polarization, before reflecting from the sample and passing through a second prism, the analyzer, to the detector. This basic setup was modified for differential measurements. The light was scanned by means of an oscillating mirror between two paths through the system; these involved reflections from separate areas of the sample surface. Optical constants were obtained by demodulation of the light-intensity fluctuations caused by polarization modulation, and the differences between the two sample areas determined by an additional demodulation at the (low) frequency of the mirror oscillation. The optical system could be maintained in the vacuum belljar in order to avoid spurious polarization induced by added optical elements. The light beam passed into the belljar

from a Xe lamp and monochromator, and was swept by the mirror prior to polarization. A microcomputer was programmed to follow the optical changes as the mirror scanned the light between the two sample halves. Figure 1 is a schematic drawing of the equipment; a detailed description is available elsewhere.[51]

In practice, small misalignments of the optical components proved important. It was necessary to perform an initial scan on a fresh Ag film each time the system was disassembled, to establish these misalignments so that correct angles could be determined and used in interpreting subsequent results. The operation also proved sensitive to the mirror-sweep amplitude, which was therefore monitored using a piezoelectric bimorph and controlled to have constant amplitude. Although quite elaborate, the resulting equipment behaved reliably in practice.[51] No other convenient method for *in situ* differential ellipsometry appears to be available.

Specimens were prepared and their properties measured in a belljar with a diffusion-pumped vacuum in the 10^{-7}-Torr range. The commercial photoelastic modulator in this work was not compatible with ultrahigh vacuum. Evaporation beams for Ag and alkali-metal deposition were obtained from stainless-steel boats and for the alloying impurity from a furnace. These were directed to a substrate of optically flat sapphire held by In in excellent thermal contact with the Cu base of a Dewar of liquid He. The sample area was maintained inside successive liquid-He and liquid-N_2 shields, apart from the open optical ports which had cooled tubes extending from the shields along the light path. Directly below the substrate was a cold shutter which could be opened for sample preparation and closed thereafter. All these precautions were taken to isolate the samples from the ambient gases in the vacuum belljar. The effect was to improve the vacuum in the immediate vicinity of the sample by perhaps 2 orders of magnitude.

Shielding for the molecular beams was so arranged that two samples were made simultaneously, and the fluxes

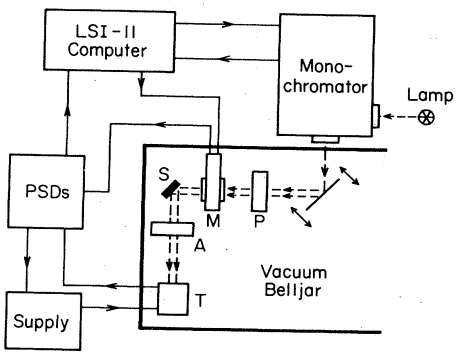

FIG. 1. Schematic of apparatus showing monochromatized light from a Xe-Hg lamp passing into the vacuum belljar, and successively passing from the sweep mirror through the polarizer *P* and the photoelastic modulator *M*. After reflecting from the sample surfaces *S*, it passes through the analyzer *A* to the phototube *T*. Schematic wiring outside the belljar indicates control and signal paths interconnecting the computer with the monochromator, modulator, demodulators, and the phototube.

measured using calibrated quartz crystals. With unity sticking coefficients at low temperature, the calculated compositions were reliable. The solvent metal was deposited on both sample areas, while, at the same time, the impurity flux reached one area only. Twin metal and alloy specimens were thus prepared together with a sharp demarcation where the impurity stopped. The mirror motion caused the optical beam to scan from one side to the other across the interface, probing the pure metal and the alloy successively.

Our practical experience is that the optical system is extremely sensitive and is easily capable of detecting the changes of optical constants caused by impurity additions below 1 at. %. The differential nature of the design contributes much to this sensitivity. In all cases, alloys were prepared from pure materials, freshly etched, and by the use of carefully out-gassed sources (the stainless-steel boat and the furnace crucible). Results nevertheless proved quite dependent on film quality. From this viewpoint the method of quench condensation, while essential for the preparation of metastable alloys, is not ideally adapted to growth of perfect films. In efforts to prepare samples based on alkali-metal host lattices, only measurements on Li-based alloys were really successful. These are reported in subsection B directly following. Brief comments about other alkali-metal-based alloys will also be found there.

Ellipsometric measurements are thus much more sensitive to film preparation than are transmission measurements of absorption.[34–36] We emphasize that the optical constants of pure-metal films such as Ag and Li could be measured with precision and were found to agree very well with the accepted results from the literature.[51] Problems with reproducibility, probably due to sample surface structure, did nevertheless occur in tests of dilute impurities in heavy alkali metals. It is unfortunate that Smith's method of examining flat alkali-metal surfaces through a transparent substrate[52] cannot be adapted easily to differential ellipsometry.

As a direct check on inconsistencies introduced by surface structure, we measured the differential reflectance of each sample directly from the optical beam intensities and compared the results with values of the differential reflectance which were calculated from the measured optical constants. Disparities between these two differential reflectance spectra were taken to signal problems caused by surface roughness, and the data were discarded. All data presented in what follows were subject to this verification procedure.

B. Results

Figure 2 shows examples of results obtained in studies of impurities in Li metal. The data are for Mg impurities in Li metal, and they represent differences between properties of pure Li films and those of the alloys. Data for three alloys of Li containing, respectively, 0.55, 5.6, and 11.5 at. % of Mg, are shown in Fig. 2. Additional results are shown in composite figures given later. In panel (a) of Fig. 2 optical-absorption spectra are measured. Panels (b) and (c) show, respectively, the real part of the optical dielectric constant, and the differential reflectance defined

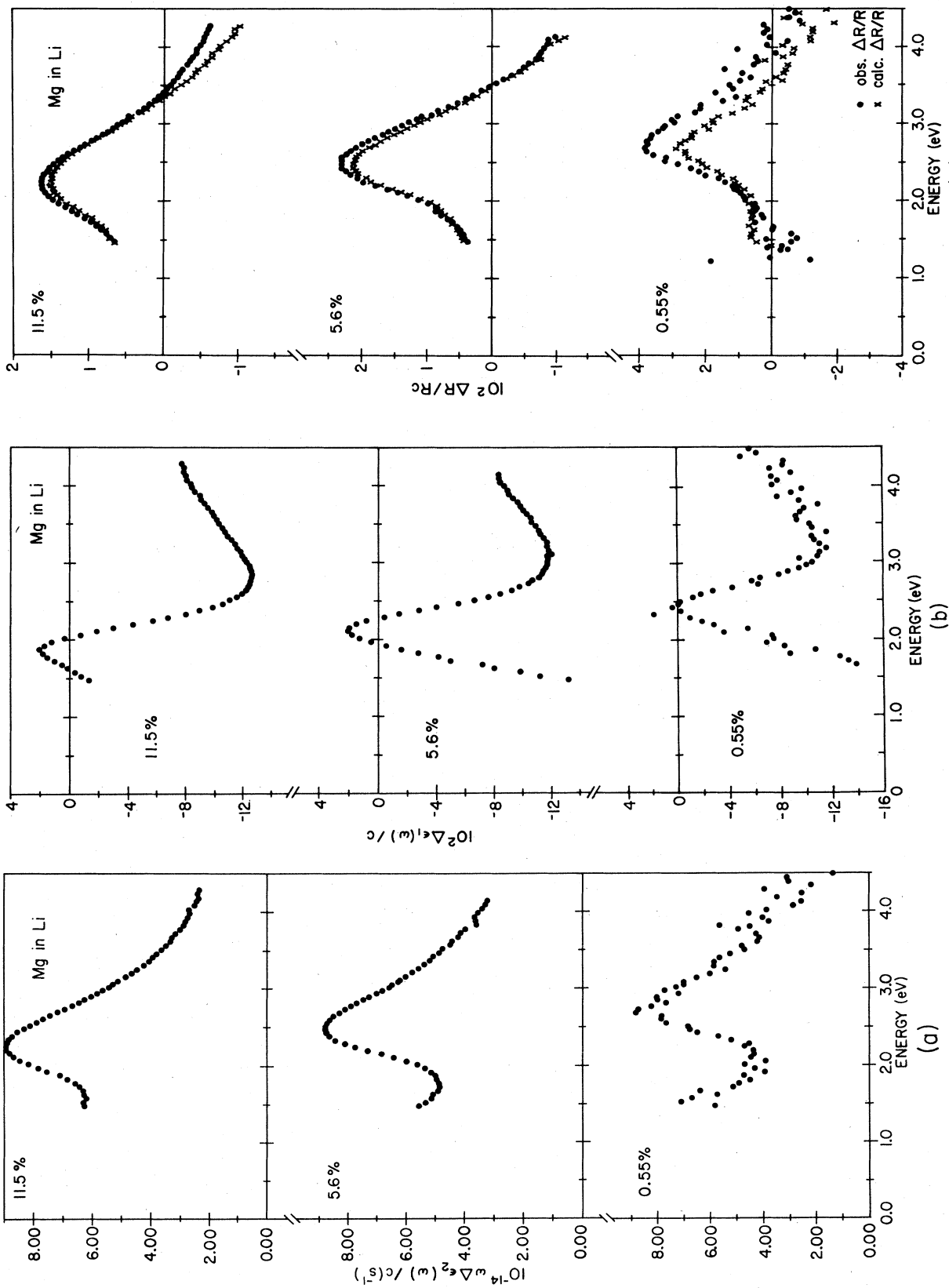

FIG. 2. Changes of optical constants at liquid-He temperature caused by small additions of Mg impurities (concentrations in at. %) to Li metal. Panel (a) gives the optical-conductivity changes scaled by the impurity concentration for easy comparison of dilute properties. Panel (b) shows the dispersive behavior for the same alloys, similarly scaled. In panel (c) the observed differential reflectivity change is compared with that deduced from the optical constants, as a check on the measurement method.

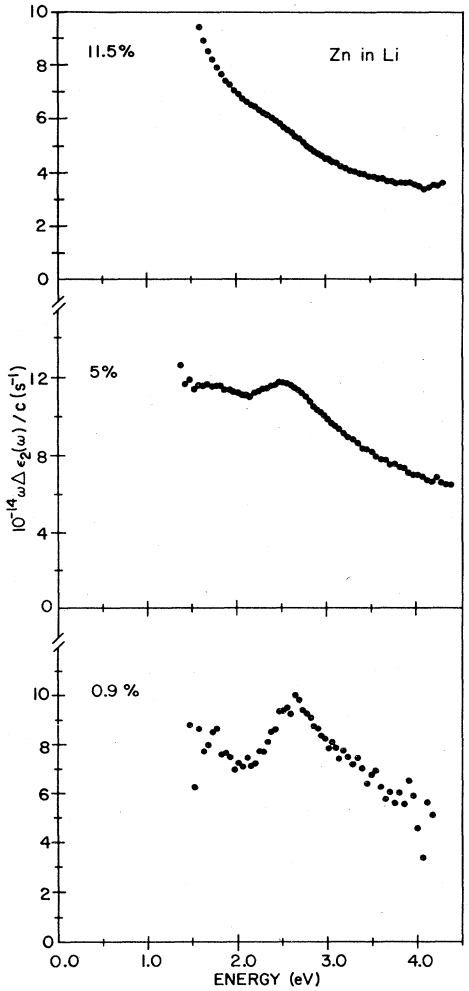

FIG. 3. Changes of optical conductivity at liquid-He temperature caused by small additions of Zn impurities to Li metal.

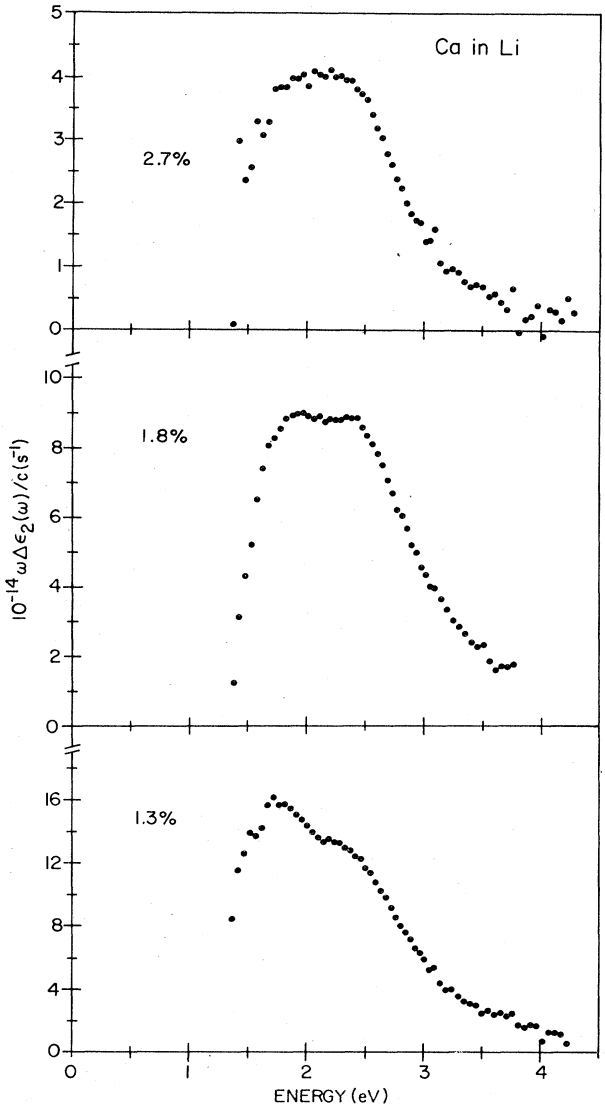

FIG. 4. Changes of optical conductivity at liquid-He temperature caused by small additions of Ca impurities to Li metal.

as the fractional change in reflectivity between the pure-metal and alloy samples.

As mentioned in subsection A above, the reflectivity provides a check on film quality. Two sets of data are shown in panel (c) for each alloy. The solid circles indicate directly measured reflectivities, while the crosses are values calculated from the measured ϵ_1 and ϵ_2. All data in all figures are scaled by the impurity concentration c to yield quantities per unit impurity content. This does not influence the comparison between directly measured and calculated reflectivities. The two sets of data are in quite good agreement, even for the 0.55-at. % alloy, where the differential effects are small and the potential for errors introduced by roughness accordingly large. The results indicate that the values of ϵ_1 and ϵ_2 are representative of the alloy rather than its surface roughness.

With the consistency of the results now checked, we turn to a discussion of ϵ_1 and ϵ_2. The optical conductivity in Fig. 2(a) shows a peak which red-shifts by about 0.5 eV in passing from 0.55 to 11.5 at. % Mg. The peak height is rather constant from one alloy to the next, however. The most dilute alloy shows that the peak is on a background which decreases rapidly as the photon energy increases, and this is confirmed for the alloy at 5.6 at. %. We interpret the background as Drude absorption, which clearly scales in proportion to Mg content as it should in the dilute limit. The peak also maintains a proportionality between size and Mg content, but it evidently shifts to progressively lower energy with increasing Mg content.

The spectra of ϵ_1 in Fig. 2(b) are presumably related to the ϵ_2 in Fig. 2(a) by the Kramers-Kronig transformation. This cannot be confirmed directly, however, because the transformation requires integrals over ω from zero to infinity. We show in Sec. III that the composite data for ϵ_1 and ϵ_2 can be fitted fairly well by a superposition of Drude terms with a second component, which is the local excitation peak, in which the contributions to ϵ_1 are indeed the Kramers-Kronig transform of those in ϵ_2.

Figures 3 and 4 show representative measurements of optical absorption for Zn and Ca in Li metal. More data

are collected below. The results for ϵ_1 and reflectivity are consistent with ϵ_2 and are not reproduced here. At 0.9 at. %, the Zn spectrum resembles that of Mg, except that there is larger Drude absorption and a smaller peak. With increasing Zn content the behavior becomes markedly different as the Drude absorption increases slightly while the peak is suppressed. At 5 at. % the peak remains clearly visible, while at 11.5 at. % it is merely a slope change on the Drude background. The Ca spectra in Fig. 4 also show a peak which decreases markedly with increasing concentration. The peak appears clearly double in all scans, and lies at lower energy, so that the Drude absorption cannot be distinguished separately. More Zn spectra are presented in a composite figure in Sec. III.

Experiments were also attempted with Mg and Zn in other alkali-metal host lattices including Cs. These were difficult, and the results proved relatively irreproducible; they will not be reported here in detail. We mention that impurity-specific features were observed for Mg in Cs metal, with a broad peak having its maximum at or above 5 eV. It seems possible that the use of more advanced techniques to improve sample control could make a much wider variety of systems accessible.

III. DISCUSSION

Our purpose in this section is to analyze and interpret the experimental results reported above. The optical excitation spectra we observe must, in part, be interpreted by comparison with theoretical models. Some aspects are clarified in paper II which follows,[1] and reference is made in this discussion to the calculations reported there. Certain features of the behavior can nevertheless be clarified directly from the systematics of the experimental results. This effort is worthwhile because it frees the interpretation from dependence on specific theories.

The fact that an independent experimental interpretation is available has determined the organization of this section. We first consider the systematic persistence of spectral features as the alloy composition is changed. This leads in successive sections to specific comments about the dilute-impurity limit, interaction effects among neighboring impurities, and, finally, about the spectra of pure divalent metals.

A. Spectral persistence

Figure 5 shows the optical conductivity of dilute Mg-Li alloys, as determined in the present experiments, together with the results of Matthewson and Myers[13] (MM) for alloys containing higher Mg concentration. In order to emphasize the continuity of the results, we have performed the necessary subtractions for the MM 18- and 30-at. % alloys, to obtain the *change* in optical conductivity from that of pure Li metal, which is what our dilute-alloy data also represent. The MM data are for annealed alloys at 200 K, whereas ours are for quench-condensed alloys at liquid-He temperature. A lack of perfect continuity between the two data sets is therefore not unexpected; for example, MM document peak shifts ≤ 0.1 eV and peak-height changes of 25% between 140 K and room temperature. In fact, a small offset would be required between the scales to prevent overlap between the two data sets. Taking the data as a whole, however, we find excellent apparent consistency between the two sets. They show that the difference spectrum contains a single dominant peak which shifts gradually from near 2.8 eV in the dilute-Mg limit to about 0.75 eV as the Mg content is increased to 100 at. %.[13,16,18]

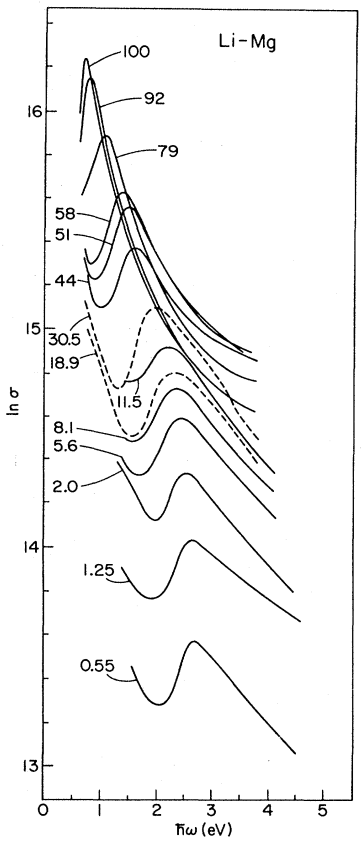

FIG. 5. Optical conductivity σ of Li-Mg alloys as a function of concentration (at. %). The data containing 18.9 at. % or more Mg are from Mathewson and Myers (MM), and the remainder are from the present research. The latter show conductivity *changes* caused by the Mg additions. Dashed curves at 18.9 and 30.5 at. % also show changes of σ according to our subtractions from MM data; for higher concentrations the difference between absolute and differential σ is small. The composite data show the conductivity peak shifting smoothly from pure Mg metal to the dilute alloy of Mg in Li metal, and with almost constant amplitude per Mg atom. Note that small amplitude and energy shifts would be needed to bring the two sets of data into full mutual consistency. These shifts are probably consequences of the different measuring temperatures and specimen-preparation conditions used in the two sets of experiments.

Because this is one of the most important aspects of the present investigation, we shall consider two alternative viewpoints on the behavior. Figure 6 shows the *total* (rather than the difference from Li) conductivity of the same series of alloys from 0 to 11 at. % Mg from the present results. The data again exhibit a satisfactory mutual consistency with the published MM results for more

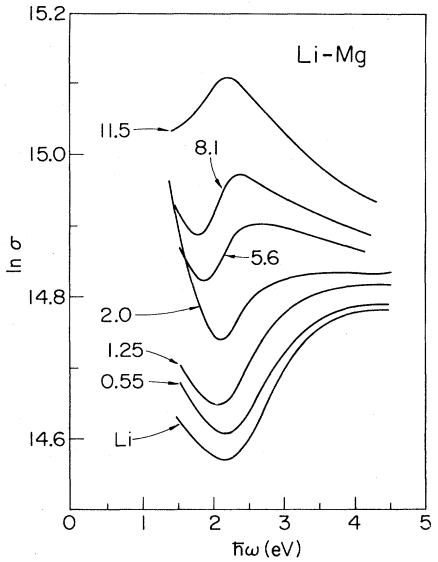

FIG. 6. Absolute optical conductivity σ of dilute Li-Mg alloys investigated in this research. Note that systematic shifts without shape change, which appear clearly in the differential results of Fig. 5, are completely lacking in the total conductivities. Instead, the shape and character of the optical response changes completely over the composition range shown.

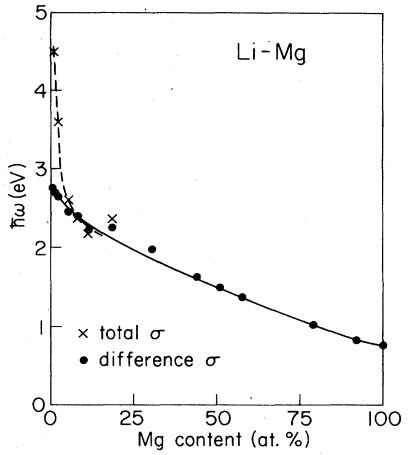

FIG. 7. Location of peak in optical conductivity σ as a function of composition in Li-Mg alloys. Solid circles show the peak of the difference curve (Fig. 5), and crosses show the peak in the total σ. The former exhibits the much smoother behavior.

concentrated alloys, given the rather different specimen conditions, but an offset between the two data sets would be needed once more to avoid overlap. For pure Li metal the peak near 4 eV is known as the interband transition, as is the 0.7-eV peak of pure Mg metal. There is a systematic evolution of the spectrum from pure Li metal to pure Mg metal as the composition changes.

A question critical to the entire experimental interpretation remains to be answered, namely: Is the peak in Fig. 5 simply the interband transition of the alloy, which shifts smoothly from that for Li to that for Mg as the number of electrons increases with increasing Mg content, or, alternatively, is it a Mg-specific contribution to the spectrum, which overwhelms the Li interband process with increasing Mg concentration, and which merges smoothly into the response of pure Mg metal, as suggested in Fig. 5? Fortunately, it appears that a choice between these alternatives can be made with good confidence.

There are four systematic features of the data themselves which affirm that the behavior in the alloys is largely Mg-specific. First, as shown in Fig. 7, the conductivity peak in Fig. 5 varies very smoothly with Mg content. Second, the strength of the peak seems to be approximately proportional to Mg concentration. Rather than resting this deduction on difficult Drude subtractions, we merely note that the peak-height variation of a factor about 3×10^2 is caused by a concentration change of about 2×10^2 (from 100 to 0.5 at. % Mg), and the peak clearly must continue to decrease linearly with concentration thereafter. It is therefore quite Mg-specific. Third, the shape of the subtracted optical response in Fig. 5 is remarkably independent of composition. It is true that the data in very-Mg-rich alloys exhibit a sharper peak and a curved tail on the logarithmic plot, but the results near 50 at. % Mg still resemble those at 0.5 at. % Mg very strongly. Fourth and finally, the strongest argument comes from the continuity of the subtracted response. Suppose for the moment that the total conductivities for a particular concentration c *did,* contrary to our belief, merely comprise a Drude portion $D_c(\omega)$ added to an interband portion $I_c(\omega)$. Then the subtracted conductivity would take the form

$$\Delta\sigma(\omega)=D_c(\omega)-D_0(\omega)+I_c(\omega)-I_0(\omega)\ ,$$

where the subscripts 0 refer to pure Li metal. The point of critical interest is that, for all low concentrations, $\Delta\sigma$ is extremely smooth (actually a linear variation on the logarithmic plot of Fig. 5) from small ω, where D_c-D_0 dominates, through the transition region to high ω, where I_c-I_0 dominates. It is exceedingly improbable that the variation of $\Delta\sigma$ would be so smooth if, as hypothesized in this argument, D and I were separately related to independent processes of Drude and interband absorption, respectively.

All these features of scaling and continuity are missing from the curves in Fig. 6, which shows *total* absorption. The peak position varies in a relatively unexpected manner (dashed line in Fig. 7), the peak strength shows no simple scaling behavior, and, of course, its shape changes in a way characteristic of the superposition of two neighboring peaks rather than a single, smoothly shifting mechanism.

In accordance with these experimental results, we therefore conclude that the Li-Mg data point unambiguously to a Mg-specific conductivity peak which grows and shifts smoothly with Mg content. The results are not consistent with the alternative of the shift and growth of an interband process. This conclusion is restricted to the Li-Mg system alone because the Li-Zn and Li-Ca systems in our work exhibit a different systematic behavior. The similarities between the Zn, Ca, and Mg results for $c\rightarrow0$ nevertheless encourage a belief that all three conductivity

peaks are impurity-specific in the dilute limit. The differences, as the concentration is increased, evidently occur for other reasons. The behavior in the dilute limit is discussed in the following subsection, and a discussion of the behavior in concentrated alloys is deferred to subsections C and D. We note here, for completeness, that behavior entirely analogous to that of Li-Mg has been previously reported[12,14] for Ag-Cd and Ag-Mg. Its origins in impurity-specific phenomena have not, however, been recognized.

B. Dilute limit

In the dilute limit, spectra are characterized by amplitudes proportional to the impurity concentration. This occurs when each impurity contributes independently, with negligible interaction effects. Behavior of this type has been observed previously in a number of systems containing transition-metal impurities.[41–45] In the present data for divalent impurities in Li metal, the spectra exhibit a linear variation with c up to about 5 at. % for Mg and about 2.5 at. % for Zn. A series of Zn spectra shown on a logarithmic scale in Fig. 8 seem to be a little erratic in absolute size, but clearly show the decay of the Zn peak. For Ca (Fig. 4) no reliable dilute limit was identified, but it evidently must exist at $c \leq 1$ at. %. Note that the Drude and impurity-specific portions of the optical response must both exhibit features appropriate to the dilute limit. The stability of both components, which gives a fixed relative line shape, as in Fig. 2 for Mg, is therefore expected. Absorption components originating in different physical processes may, however, depart from dilute-limit behavior at differing upper concentrations.

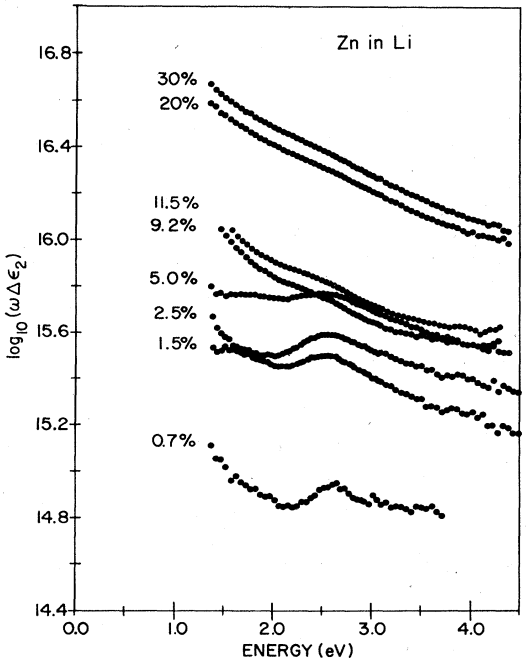

FIG. 8. Optical conductivity for Li-Zn alloys at liquid-He temperature as a function of Zn concentration (in at. %). Note that the peak 2.5 eV evident for the dilute materials becomes submerged in the Drude background for alloys above about 10 at. % Zn.

The spectra for Mg, Zn, and Ca differ significantly among themselves. We establish in Sec. III A that the spectral profile for Mg is impurity-specific and is not related to interband transitions of the "average" alloy. This very probably holds true for Zn and Ca also, although the arguments which affirm the deduction for Mg no longer apply for Zn and Ca because the profiles change with composition such that the peaks become submerged in the Drude background. The sharp structure at dilution for Zn is, however, very similar in shape and position to that of Mg. Spectra for pure Zn exhibit a sharp peak near 1.6 eV and a spin-orbit shoulder at 1.2 eV,[5,22–25] but the connection between these and the spectrum for 10 at. % Zn in Li is not yet established. In the case of Ca, the profile is somewhat different. However, the doublet structure which can be detected in all three scans of the Ca peak in Fig. 4 appears to be Ca-specific. The spin-orbit splitting of the $4s\,4p\,(P_{3/2},P_{1/2})$ states in the free atom is 0.97 eV,[47] which is in the same range as the apparent splitting of about 0.50 eV in the Ca impurity spectra. Accordingly, there is reason to believe that the differences among the spectra of Mg, Zn, and Ca in the dilute limit are impurity-specific and relate to differences among the electronic structures of the impurities.

The three impurity spectra differ in both the apparent ratio of the Drude-continuum component to the peaked component and in the positions of the peaks themselves. For Zn the continuum is largest and the peak is weak, whereas for Ca the continuum is low and not clearly identifiable in the spectral range shown in Fig. 4. Overall, however, the spectra show comparable oscillator strengths, as indeed is necessary if they are to exhaust their respective $ns^2 \rightarrow nsnp$ transition strengths. It is clear that the emergence of visible peak structure depends not only on the existence of sharp features, but also on the availability of adequate oscillator strength in excess of the contribution of elastic scattering, which appears as the Drude continuum.

With regard to the peak positions, we note that the peak maxima are located at 2.8 eV for Mg and 2.6 eV for Zn. The Ca peaks occur at about 1.7 and 2.2 eV. Cluster calculations described in paper II provide a detailed description of impurity-specific excitations of Mg and Zn in Li metal.[1] The calculations show that the electron and hole localize together on the impurity site. The energy of the excited configuration is calculated to be 2.75 eV for Mg in Li metal and 2.48 eV for Zn in Li metal. No calculated results are available for Ca in Li metal, but the atomic spin-orbit splitting is comparable with that observed in the alloy, as mentioned above. These results all indicate very good agreement between the observations and the impurity-specific model we have proposed to describe the results.

At present, no comprehensive theory is available by which the shape of the absorption peak can be interpreted. It is of interest to see how well the dielectric response can be represented by a model superposition of Drude and local behavior. Figure 9 shows a best fit to the Mg-conductivity, dispersion, and reflectivity results obtained

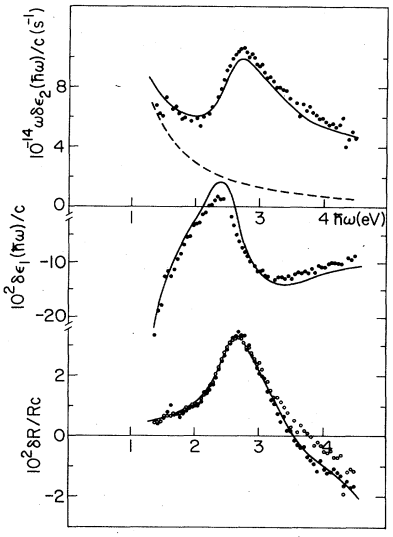

FIG. 9. Separation of differential optical response into Drude and local components for an alloy of 1.25 at. % Mg in Li metal. The dashed line shows the assumed Drude $\epsilon_2(\omega)$ and the solid line shows the result when a chosen local term is added. The local response is constrained to give solely positive contributions. The lower curves show dispersion and reflectivity calculations (solid lines) obtained by Kramers-Kronig transformation. It is possible that, in reality, the local contribution interferes with the Drude continuum.

by summing Drude terms with an excess portion chosen to represent the excitonic resonance at the impurity. For specific modeling, the local term was constrained to give positive absorption only. A Kramers-Kronig transform of the assumed absorption, with appropriately weak and smooth behavior in the wings, was used to obtain $\epsilon_1(\omega)$. It was found that no perfect fit could be obtained, even with the two rather weak constraints of the Drude form and the requirement of positive local absorption. Nevertheless, the "best" fit to the overall behavior is reasonably good. The fit is obtained with Drude scattering corresponding to a residual resistivity of about 3 $\mu\Omega$ cm/at. %, which may be compared with the observed values of 1.4 $\mu\Omega$ cm/at. %.[53]

It is quite possible that the continuum and local absorption do not superpose but, rather, may, in part, interfere. Figure 10 indicates three configurations of the metal-impurity complex. In Fig. 10(a) the metal is in its ground state and the Mg $3s$ orbitals are both occupied. The Mg $3s\,3p$ configuration obtained by photon absorption is shown in Fig. 10(b), with the metal still in its ground state (no electron-hole excitations). Figure 10(c) shows the complex with the Mg returned to the $3s^2$ configuration and its excitation energy passed to the conduction electrons. This corresponds to an Auger-like decay[54] of the locally excited state into conduction-band excitations. The point is, however, that the state depicted in panel (c) is directly accessible by photon absorption also, and indeed such processes constitute the Drude continuum of the metallic absorption.[55] However, the states depicted in panels (b) and (c) are assuredly coupled by decay through Coulomb matrix elements. It follows that the two absorption processes may interfere as in the Fano[56] resonances of atomic autoionizing excitations.[57] It is precisely this type of behavior, with Fano-like profiles, that has been reported for the $3d^{10}4s^2 \rightarrow 3d^9 4s^2 4p$ excitations of Zn impurities and adsorbates with alkali-metal hosts.[54] The present $s^2 \rightarrow sp$ excitations lead to much the same final valence configuration, so that the occurrence of interferences in the observed profiles appears very likely. We anticipate that a complete eventual description of the impurity-specific line shapes will indeed involve interference effects of this type.

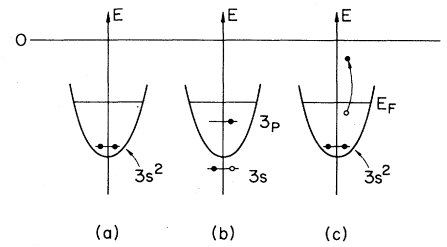

FIG. 10. The Mg $3s^2$ ground state is shown in panel (a), and the excited $3s\,3p$ configuration is shown in (b). A band excitation degenerate with (b) is shown in (c). The observed line shape may result from an interference between (b) and (c).

In summary of the results for the dilute limit, one may note that the observed peaks agree well with predictions for the excitonic resonance. At present, no comprehensive theory of the spectral profile is available. It appears, probably, that a correct theory must include interference between local and continuum processes.

C. Interaction effects

Figures 5—8 clearly show that the impurity spectra shift and change shape with impurity concentration. Ca has the most striking effects, with the peak decreasing rapidly in height as the concentration is increased. For Zn the changes are hardly less dramatic since the peak vanishes into the Drude continuum when the impurity content is raised to ~ 10 at. %. In the case of Mg, the peak persists with undiminished strength per atom, but shifts smoothly in position, as shown in Figs. 5 and 7. Here we present a brief discussion of these effects and the processes that underlie them.

Sections III A and III B collect evidence that the optical peaks correspond to processes localized at impurities in the lattice. Most specifically, they mark excitonic resonances in which s-like holes and p-like electronic states are trapped at an impurity under the joint influence of their mutual interaction and the impurity field. Given metallic screening, the influence of an impurity on the neighboring lattice hardly extends beyond near-neighboring sites (see, for example, paper II). This is also true for an excited impurity, which simply acts as a chemically different impurity (in the "$Z+1$ model," which often represents chemical bonding very successfully,[35] the excited Mg impurity resembles the ground state of dissolved Al, for example). In view of the short range of the interactions, it seems reasonable to discuss spectral shifts of the excitonic resonances in terms of the immediate lo-

cal environment and its influence on the excitation.

To see how this works out, we note that, in a system in which each atom has ν nearest neighbors, the probability that a particular impurity has *no* near-neighbor impurities is $(1-c)^{\nu}\simeq\exp(-\nu c)$. Thus, half of the impurities remain unperturbed when $c=0.07$ for $\nu=10$, but at $c=0.07$ the Zn peak is reduced by roughly a factor of 2 in relative amplitude. This seems to indicate that one or more Zn near neighbors suffices to largely eliminate the peaked response of any Zn impurity in Li. For Ca it seems that a Ca atom in either of the first two neighboring shells causes major spectral changes. Mg impurities have milder interaction effects. By 5 at. % the linear region in the dilute limit is terminating, as the peak is then significantly shifted to lower energies, although other changes are small. Evidently, Mg neighbors cause the Mg excitation to red-shift.

It is interesting to see how these interaction effects are reproduced, in part, by cluster calculations in which two impurities at neighboring sites are embedded in a surrounding cluster of Li metal. Details of the calculation are provided in paper II.[1] As expected, an optical excitation on one member of an impurity pair can resonate between the two sites. Its energy is then "tunnel-split" into a bonding and antibonding pair which occur on either side of the central impurity line. The cluster calculations reported in paper II show that the Mg tunnel splitting is $\epsilon\simeq0.16$ eV. For 10 neighbors one would expect a shift $\Delta E\simeq-10\times\frac{1}{2}\times0.16\simeq-0.8$ eV of the symmetric (optical) combination. The observed peak shift is ~-2 eV from Li to Mg. For Zn in Li, on the other hand, the calculated splitting is $\epsilon\simeq0.73$ eV. This is a large shift, which indicates that the Zn peak will spread rapidly as the Zn concentration is increased. It is likely that the inhomogeneous broadening associated with combinations of such splittings causes the disappearance of the Zn peak near 5 at. % Zn. The fact that the splitting is much smaller for Mg may permit the average Mg peak to shift smoothly with composition, without too strong a broadening caused by differences between one site and the next.

The precision afforded by the differential methods used here makes the present results particularly informative about impurity-specific contributions to alloy adsorption spectra. Fortunately, however, there are other data which bear on these same phenomena. By the nature of the measurement method employed, these mostly provide information about alloys in the more concentrated regime. The following brief comments are confined to the case of divalent impurities in order to make full contact with the issues addressed in this paper.

Of particular interest are results for Ag-Mg (Ref. 14) and Ag-Cd (Refs. 12 and 14) alloys. Results are also available for Cu-Zn,[15] but the main shallow features appear to be dominated by $3d$-band behavior. This is not the case for Ag alloys, where $4d$-band excitations occur above 4 eV, beyond the range of interest for $5s^2\rightarrow5s\,5p$ excitations. Green and Muldawer,[12] and Flaten and Stern,[14] have examined several alloys in the range 2—40 at. % Cd in Ag and 4—30 at. % Mg in Ag, to obtain $\epsilon_2(\omega)$ between about 1.5 and 5.5 eV. In both cases a large peak grows and shifts with impurity content. In Ag, the Mg and Cd peaks for the dilute limit both appear to be centered a little above 4 eV, just as Mg, Zn, and Ca all occur between 2 and 3 eV in Li metal. This is a point of special interest in the theory (see paper II). Furthermore, the shift of the peak with increasing concentration occurs much as in Li-Mg, so that the peak position extrapolates for $c=100$ at. % towards the main optical-absorption peak of the pure divalent metal. Like the Li-Mg results, these data from the literature have been interpreted by earlier workers in terms of band properties; they, also, are much better suited to interpretation through excitonic resonance behavior. Careful investigation of the dilute regime in these systems will, however, be required to establish our alternative explanation in a definitive way.

To summarize this section we note that the behavior of the Mg, Zn, and Ca spectra in Li metal are consistent with a model in which the excitonic resonance is progressively more perturbed by neighboring impurities as the concentration is increased. The magnitudes of the neighbor-induced shifts for Mg and Zn are in semiquantitative agreement with the results of cluster calculations described in paper II. We note that other data in the literature for alloys containing divalent impurities exhibit very similar trends of spectral persistence. These warrant further investigation to establish a definitive interpretation of the impurity response at the dilute limit.

D. Pure divalent metals

Experimental investigations of the pure divalent metals[16–25] have revealed characteristically sharp, low-energy peaks, with clear spin-orbit splittings for the heavier elements. The peaks are known as the interband transitions at the Brillouin-zone faces. These effects are expected to occur for divalent elements, in which the electrons exactly fill the first zone apart from a small spillover which depends on the size of the band gap. It is this excess of free electrons and holes that distinguishes the electronic structure of the metals from that, for example, of He, where the lowest zone-boundary excitation is an exciton.

Now the peak in the excitation spectrum of Mg-Li, which we have identified as an excitonic resonance, clearly deforms continuously into the principal excitation of the pure Mg system (see Fig. 5). Moreover, it does so without perceptible modification at the bcc-to-hcp transition near 70 at. % Mg. These two facts cast doubt on the interpretation of the peak in pure Mg as a simple interband transition. In an earlier paper[49,10] we propose, instead, that the interband transition exhibits strong resonance excitonic enhancement, so that band-structure details other than the gap exert only a weak influence on the spectrum. Contrary proposals have been forthcoming,[58] but it appears probable to us that the electron-hole interaction does indeed play a strong role in determining the response.

One should bear in mind that the interband transition at the zone boundary has much in common with our proposed resonance behavior, in which the Mg $3s^2\rightarrow3s\,3p$ *local* excitation interacts with the conduction-electron excitation continuum.[48,49] First, the vertical excitation at the zone boundary is, in fact, a transition from $3s$- to $3p$-like

states. Second, since $\nabla_k E_k \simeq 0$ near the zone face, it follows that the two quasiparticles created in the optical process are almost stationary. A final important point is that the electron and hole are created at the same position in the lattice. In our proposed mechanism, the *s* hole and *p* electron of the interband transition, being slowly moving and created close together, interact through short-range forces to form a coupled structure which persists for some brief interval. In conventional band calculations, on the other hand, all dynamical effects of the interaction between the quasiparticles are neglected. The band-theory calculation is therefore the limiting case of the excitonic behavior in which the interactions causing enhancement are set to zero.

These views have prompted Kunz and Flynn[10] to propose a theory in which the vertical electron-hole—pair states of independent-particle theory are used as basis functions through which the behavior of interacting particles can be treated. Upon exactly diagonalizing the problem for short-range interactions between the quasiparticles, these workers find new wave functions that depend on the strength of the interaction. It turns out that the spectral response is strongly modified for moderate interactions of, say, 1 eV, and changes continuously to about 4.5 eV, where an excitonic bound state forms. The enhancement dominates the response in such a way that the observed spectral response of Mg is reproduced reasonably well for interaction strengths near 3 eV regardless of the detailed form of the band structure. Direct calculations yield estimates of the interaction of about 2 eV. The theory for the interacting system is therefore quite consistent with our experimental deduction that the interaction between the freshly created quasiparticles has a major effect on the optical spectrum.

Further confirmation comes from the cluster calculations reported in paper II. There we report an investigation of optical response in a cluster of 19 Mg atoms. It is found that the *p* electron *does* localize on the *s* hole in the cluster. The excitation energy of 1.2 eV obtained in these *a priori* calculations agrees very well with the observed "interband" transition of the pure Mg metal above the 0.7-eV band edge.

In conclusion, we note that the experimental evidence points clearly to the role of interactions between quasiparticles in modifying the optical response of Mg metal. The deductions are supported by both continuum treatments of the interacting system and by cluster modeling of the excited metal. It seems very probable that the excitonic resonance phenomena which these results establish for Mg metal must play an important part in the optical response of other pure divalent metals also. Similar phenomena are likely to be widespread in pure and alloyed transition metals where the conditions are also generally very favorable for low-energy excitonic resonance processes.

ACKNOWLEDGMENTS

The authors acknowledge support by the National Science Foundation (Materials Research Laboratories Program) at the University of Illinois under Grant No. DMR-83-16981.

[1]J. C. Boisvert, P. W. Goalwin, A. B. Kunz, M. H. Bakshi, and C. P. Flynn, following paper, Phys. Rev. B **31**, 4984 (1985).
[2]Y. Frenkel, Phys. Rev. **37**, 17 (1931); **37**, 1276 (1931).
[3]G. H. Wannier, Phys. Rev. **52**, 191 (1937).
[4]R. S. Knox, in *Theory of Excitons,* Suppl. 5 of *Solid State Physics,* edited by F. Seitz and D. Turnbull (Academic, New York, 1963).
[5]J. C. Phillips, in *Solid State Physics,* edited by F. Seitz and D. Turnbull (Academic, New York, 1966), Vol. 18.
[6]R. J. Elliott, Phys. Rev. **108**, 1384 (1957).
[7]M. M. Cohen and J. C. Phillips, Phys. Rev. Lett. **12**, 662 (1964).
[8]G. D. Mahan, Phys. Rev. Lett. **18**, 448 (1967).
[9]V. Vinter, Phys. Rev. Lett. **35**, 598 (1975); H. Drew and M. Verdun, *ibid.* **33**, 1608 (1974).
[10]A. B. Kunz and C. P. Flynn, Phys. Rev. Lett. **50**, 1524 (1983).
[11]M. S. Miller and H. D. Drew, J. Phys. F **13**, 1885 (1983).
[12]E. L. Green and L. Muldawer, Phys. Rev. B **2**, 330 (1970).
[13]A. G. Mathewson and H. P. Myers, J. Phys. F **3**, 623 (1973).
[14]C. J. Flaten and E. A. Stern, Phys. Rev. B **11**, 638 (1975).
[15]See various papers in *Optical Properties and Electronic Structure of Metals and Alloys,* edited by F. Abeles (North-Holland, Amsterdam, 1966).
[16]D. Jones and A. M. Lettington, Proc. Phys. Soc. London **92**, 948 (1967).
[17]J. B. Ketterson and R. W. Stark, Phys. Rev. **156**, 748 (1967).
[18]R. H. W. Graves and A. P. Lenham, J. Opt. Soc. Am. **58**, 126 (1968).
[19]O. Hunderi, J. Phys. F **6**, 1223 (1976); A. G. Mathewson and H. P. Myers, Phys. Scr. **4**, 291 (1971).
[20]P. O. Nilsson and G. Forssell, Phys. Rev. B **16**, 3352 (1977).
[21]L. P. Mosteller and F. Wooten, Phys. Rev. **171**, 743 (1968).
[22]J. H. Weaver, D. W. Lynch, and R. Rosei, Phys. Rev. B **5**, 2829 (1972).
[23]G. W. Rubloff, Phys. Rev. B **3**, 285 (1971).
[24]W. R. S. Garton and J. P. Connrade, Astrophys. J. **155**, 667 (1969).
[25]O. Hunderi and H. P. Myers, J. Phys. F **4**, 1088 (1974).
[26]P. O. Nilsson, in *Solid State Physics,* edited by F. Seitz, D. Turnbull, and H. Ehrenreich (Academic, New York, 1974), Vol. 29.
[27]H. Ehrenreich and L. M. Schwartz, in *Solid State Physics,* edited by F. Seitz, D. Turnbull, and H. Ehrenreich (Academic, New York, 1976), Vol. 31.
[28]D. J. Sellmyer, in *Solid State Physics,* edited by H. Ehrenreich, F. Seitz, and D. Turnbull (Academic, New York, 1978), Vol. 33.
[29]P. M. Soven, Phys. Rev. **151**, 539 (1966); **156**, 809 (1967).
[30]See, for example, S. Kirkpatrick, B. Velický, and H. Ehrenreich, Phys. Rev. B **1**, 3250 (1970); K. Levin and H. Ehrenreich, *ibid.* **3**, 4172 (1971).
[31]G. D. Mahan, in *Solid State Physics,* Ref. 26.
[32]G. D. Mahan, Phys. Rev. **163**, 612 (1967).
[33]P. Nozières and C. T. DeDominicis, Phys. Rev. **178**, 1097 (1969).
[34]R. Avci and C. P. Flynn, Phys. Rev. B **19**, 5967 (1979); **19**, 5981 (1979).
[35]D. J. Phelps, R. A. Tilton, and C. P. Flynn, Phys. Rev. B **14**,

5254 (1976); **14**, 5265 (1976); **14**, 5279 (1976).
[36]T. H. Chiu, D. Gibbs, J. E. Cunningham, and C. P. Flynn, J. Phys. F **13**, L23 (1983).
[37]Much the same comments apply to adsorbates; see J. E. Cunningham, D. Gibbs, T. H. Chiu, and C. P. Flynn, J. Phys. C **14**, L1113 (1981).
[38]P. W. Anderson, Phys. Rev. **124**, 41 (1961).
[39]B. Caroli, Phys. Kondens. Mater. **1**, 346 (1963).
[40]B. Kjollerstrom, Philos. Mag. **19**, 1207 (1969).
[41]H. P. Myers, L. Wallden, and A. Karlsson, Philos. Mag. **18**, 725 (1968).
[42]M. R. Steel and D. M. Trehern, J. Phys. F **2**, 199 (1972).
[43]A. B. Callender and S. E. Schnatterly, Phys. Rev. B **7**, 4385 (1973).
[44]M. D. Drew and R. E. Doezema, Phys. Rev. Lett. **28**, 1581 (1972).
[45]D. Beaglehole, Phys. Rev. B **14**, 341 (1976).
[46]W. L. Wiese, M. W. Smith, and B. M. Glennon, *Atomic Transition Probabilities* [U.S. National Bureau of Standards, Washington, D.C., 1966 (Vol. 1) and 1969 (Vol. II)].
[47]C. E. Moore, *Atomic Energy Levels* (U.S. National Bureau of Standards, Washington, D.C., 1971).
[48]G. Denton, M. Bakshi, and C. P. Flynn, Phys. Rev. B **26**, 3495 (1982).
[49]M. Bakshi, G. A. Denton, A. B. Kunz, and C. P. Flynn, J. Phys. F **12**, L235 (1982).
[50]S. N. Jasperson and S. E. Schnatterly, Rev. Sci. Instrum. **40**, 761 (1969); S. N. Jasperson, D. K. Burge, and R. C. O'Handley, Surf. Sci. **37**, 548 (1973).
[51]G. A. Denton, Ph.D. thesis, Univeristy of Illinois, 1982; M. H. Bakshi, Ph.D. thesis, University of Illinois, 1984.
[52]N. V. Smith, Phys. Rev. **183**, 634 (1969).
[53]T. E. Faber, Philos. Mag. **15**, 1 (1967). The value of resistence taken for pure quench-condensed Li was from R. Avci and C. P. Flynn [Phys. Rev. B **19**, 5967 (1979)].
[54]T. H. Chiu, J. E. Cunningham, D. Gibbs, and C. P. Flynn, Phys. Rev. Lett. **52**, 388 (1984).
[55]See, e.g., J. M. Ziman, *Principles of the Theory of Solids* (Cambridge University Press, Cambridge, 1972).
[56]U. Fano, Phys. Rev. **124**, 1866 (1961); U. Fano and J. W. Cooper, Rev. Mod. Phys. **40**, 441 (1968).
[57]H. Beutler, Z. Phys. **87**, 176 (1933).
[58]G. Mula, R. Car, and S. T. Pantelides, Bull. Am. Phys. Soc. **29**, 432 (1984).